Bioorganic & Medicinal Chemistry Letters 23 (2013) 3927–3934

Contents lists available at SciVerse ScienceDirect

Bioorganic & Medicinal Chemistry Letters

journal homepage: www.elsevier.com/locate/bmcl

Novel nicotinic acetylcholine receptor agonists containing carbonyl moiety as a hydrogen bond acceptor

Anatoly A. Mazurov *, David C. Kombo, Srinivasa Akireddy, Srinivasa Murthy, Terry A. Hauser, Kristen G. Jordan, Gregory J. Gatto, Daniel Yohannes

Targacept, Inc., 100 North Main Street, Winston-Salem, NC 27101, USA

ARTICLE INFO

Article history:
Received 21 February 2013
Revised 14 April 2013
Accepted 22 April 2013
Available online 1 May 2013

Keywords:
3-Azabicyclo[3.3.1]nonane
3-Azabicyclo[3.3.0]octane
3,7-Diazabicyclo[3.3.1]nonane
3,7-Diazabicyclo[3.3.0]octane
Hydrogen bond acceptor
Nicotinic acetylcholine receptor
Novel object recognition
Selective nAChR agonist

ABSTRACT

A novel series of α4β2 nAChR agonists lacking common pyridine or its bioisosteric heterocycle have been disclosed. Essential pharmacophoric elements of the series are exocyclic carbonyl moiety as a hydrogen bond acceptor and secondary amino group within diaza- or azabicyclic scaffold. Computer modeling studies suggested that molecular shape of the ligand also contributes to promotion of agonism. Proof of concept for improving working memory performance in a novel object recognition task has been demonstrated on a representative of the series, 3-propionyl-3,7-diazabicyclo[3.3.0]octane (**34**).

Nicotinic acetylcholine receptors (nAChRs) belong to a family of ligand-gated ion channels activated by neurotransmitters and are members of the Cys-loop superfamily of receptors. At least 16 different genes code for nAChR subunits, which can assemble as pentamers in distinctive combination to form diverse nAChR subtypes. nAChRs, which are extensively distributed throughout the central (CNS) and peripheral (PNS) nervous system, regulate neuronal function by modulating release of several neurotransmitters, including acetylcholine, dopamine, serotonin and GABA. The predominant α4β2 and α7 nAChR subtypes appear to play significant roles in cognitive function, neuronal degeneration, schizophrenia, and pain.[1] Subtype-selective ligands can differentially modify or regulate the activity of corresponding nAChRs. With this in mind, designing and targeting ligands to selectively interact with a distinct nAChR receptor subtype may increase therapeutic precision, with the potential to maximize benefit and minimize adverse effects.

The prevalence of α3β4 nAChRs in the autonomic ganglia supports the hypothesis that activation of this subtype contributes to gastrointestinal and cardiovascular effects of nonselective nicotinic ligands.[2] Despite certain progress, the discovery of potent α4β2 nAChR agonists with substantial functional selectivity over α3β4 nAChRs has been a major challenge. Clinical trials with nAChR agonist **1** (Fig. 1) were discontinued due to a narrow therapeutic index.[3] Compound **2** failed to demonstrate efficacy when tested at low doses in patients with diabetic neuropathic pain.[4] Peripheral and central adverse effects of the partial α4β2 nAChR agonist **3**, a smoking cessation medicine, may also be attributed to suboptimal subtype selectivity.[5]

Most known α4β2 nAChR agonists contain a 3-pyridinyl moiety, which is thought to be a key pharmacophoric element. Despite this belief, recently we described a selective α4β2 nAChR agonist AZD1446 (**4**)[6] which lacks a pyridinyl moiety. We discovered this selective α4β2 nAChR agonist by bioisosteric replacement of the hydrogen bond acceptor pyridine with a furoyl moiety in an diazabicyclo[3.3.0]octane series. To evaluate the effect of the electronic environment on the carbonyl group as a hydrogen bond acceptor, we obtained and characterized several series of amides, carbamates, and ketones (Tables 1–3)[7] based on diazabicyclic and azabicyclic scaffolds.

Commercially available N-Boc protected 3,7-diazabicyclo[3.3.0]octane and 3,7-diazabicyclo[3.3.1]nonane were coupled with corresponding carboxylic acids or methyl chloroformate followed by deprotection to provide amides **15**–**35** and carbamates **36** and **37**. The 3-azabicyclooctane scaffold **7** (Scheme 1) was produced by reaction of allyl iodomalonate **6** and N-Boc-protected allylamine in accordance with an adapted tandem radical annulation/ionic

* Corresponding author. Tel.: +1 336 545 8010.
E-mail address: galana99@yahoo.com (A.A. Mazurov).

0960-894X/$ - see front matter © 2013 Elsevier Ltd. All rights reserved.
http://dx.doi.org/10.1016/j.bmcl.2013.04.058

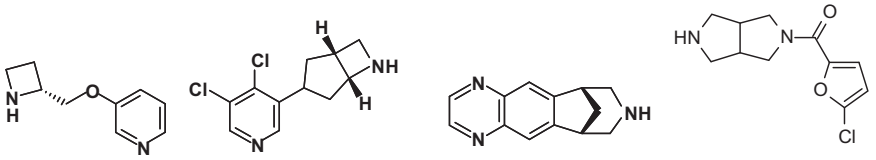

tebanicline, 1 **ABT-894, 2** **varenicline, 3** **AZD1446, 4**

Figure 1. Selected α4β2 nAChR ligands.

Table 1
Affinity and agonism of cyclopropyl carboxamides

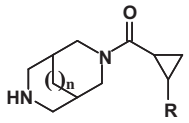

Compd	*n*	R	Configuration	Affinity, K_i			Agonism			
				h α4β2 (nM)	*h* α3β4 (μM)	*h* α7 (μM)	*h* α4β2		*h* α3β4	
							EC_{50} (μM)	E_{max} (%)	EC_{50} (μM)	E_{max} (%)
Nicotine				2 ± 0.2	0.4 ± 0.1	3 ± 0.4	3 ± 0.07	100	7 ± 0.1	100
4				30 ± 5	>10	6.7 ± 1.9	4.9 ± 0.7	120 ± 11	70 ± 12	10 ± 3
15	0	H	–	4 ± 1	0.67 ± 0.11	0.84 ± 0.16	0.47 ± 0.08	110 ± 2	4.9 ± 0.3	130 ± 3
16	0	F	1*S*,2*S*	17[a]	0.86[a]	6.9[a]	0.93 ± 0.34	120 ± 8	13[a]	88[a]
17	0	F	1*R*,2*R*	5[a]	0.38[a]	1.4[a]	1.0 ± 0.5	130 ± 15	24[a]	140[a]
18	0	F	1*R*,2*S*	30[a]	0.81[a]	2.7[a]	0.9 ± 0.1	140 ± 6	14 ± 4.6	90 ± 21
19	0	F	1*S*,2*R*	9 ± 3	0.42 ± 0.17	0.99 ± 0.39	0.19 ± 0.05	130 ± 8	8.4 ± 2.5	150 ± 12
20	0	Me	1*R*,2*S*	18[a]	2[a]	4.5[a]	19[a]	100[a]	10[a]	110[a]
21	0	Me	1*S*,2*R*	1[a]	0.28 ± 0.01	0.35[a]	1.2[a]	140[a]	1.4[a]	180[a]
22	0	Me	1*R*,2*R*	4[a]	0.36[a]	1.9[a]	1.7[a]	100[a]	14[a]	110[a]
23	0	Me	1*S*,2*S*	43[a]	13[a]	100[a]	5.6[a]	68[a]	34 ± 1.4	26 ± 2
24	1	H	–	1 ± 0	0.11 ± 0.05	0.02 ± 0.00	0.85 ± 0.14	46 ± 13	1.2 ± 0.3	160 ± 16
25	1	F	1*S*,2*S*	5.2[a]	1.2 ± 0.17	0.3[a]	0.4[a]	11[a]	11[a]	90[a]
26	1	F	1*R*,2*R*	1.4[a]	0.15[a]	0.1[a]	9.2[a]	7[a]	2.1[a]	130[a]
27	1	F	1*S*,2*R*	1[a]	0.036 ± 0.012	0.01[a]	0.43 ± 0.29	77 ± 12	0.39 ± 0.04	130 ± 6
28	1	F	1*R*,2*S*	7.3[a]	0.32[a]	0.4[a]	2.7 ± 1.6	84 ± 24	8.0 ± 4.7	210 ± 61
29	1	Me	1*R*,2*R*	1[a]	0.1[a]	0.03[a]	12[a]	23[a]	1.6[a]	120[a]
30	1	Me	1*S*,2*S*	28[a]	0.6[a]	0.3[a]	10[a]	21[a]	8.3[a]	89[a]
31	1	Me	1*S*,2*R*	0.2[a]	0.01[a]	0.005[a]	1.9[a]	5[a]	0.08[a]	160[a]
32	1	Me	1*R*,2*S*	2.9[a]	0.1[a]	0.1[a]	100[a]	0.5[a]	0.3[a]	140[a]

[a] *n* = 1.

Table 2
Affinity and agonism of aliphatic amides and carbamates

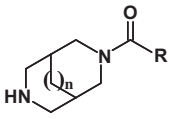

Compd	*n*	R	Affinity, K_i			Agonism			
			h α4β2 (nM)	*h* α3β4 (μM)	*h* α7 (μM)	*h* α4β2		*h* α3β4	
						EC_{50} (μM)	E_{max} (%)	EC_{50} (μM)	E_{max} (%)
33	0	Me	38[a]	14[a]	ND[b]	2.6[a]	110[a]	23[a]	36[a]
34	0	Et	12[a]	2.1[a]	4[a]	1.3 ± 0.4	120 ± 9	18 ± 2.5	130 ± 5
35	1	Me	20[a]	5.5[a]	3.3[a]	9.9 ± 0.6	34 ± 6	13[a]	110[a]
36	1	Et	8 ± 2	20[a]	1.6[a]	1.9 ± 0.1	83 ± 7	5.9 ± 4.5	130 ± 9
37	1	OMe	20[a]	ND	ND	5.2[a]	65[a]	ND	ND
38	0	OMe	23[a]	14[a]	ND	ND	ND	16 ± 6	85±11

[a] *n* = 1.
[b] ND = not determined.

cyclization sequence.[8] Halogen atom transfer annulation was performed in situ by an addition of triethylamine after iodine abstraction from **6** under nonreducing radical generating conditions and intermolecular addition to the acceptor olefin. Decarboxylation of **7** in refluxing hydrochloric acid followed by protection of the amino group provided 7-carboxy-3-azabicyclooctane **8** as a mixture of *cis*- and *trans*-isomers. Geometrical isomerism of the 7-substituted 3-azabicyclooctane is driven by a different orientation of the substituent and the fused pyrrolidine ring. Amino acid **8** was applied for the synthesis of ketones **39** and 4**0** via Weinreb amide **9**,[9]

Table 3
Affinity and agonism of azabicyclic derivatives

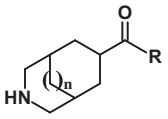

Compd	*n*	R	Affinity, K_i			Agonism			
			h α4β2 (nM)	*h* α3β4 (μM)	*h* α7 (μM)	*h* α4β2		*h* α3β4	
						EC_{50} (μM)	E_{max} (%)	EC_{50} (μM)	E_{max} (%)
39	0	Cyclopropyl	0.5 ± 0.0	0.07[a]	0.14[a]	0.018 ± 0.007	120 ± 8	0.93 ± 0.47	130 ± 18
40	0	2-Furyl	13[a]	2.2[a]	3.4[a]	1.6 ± 0.6	94 ± 10	11[a]	40[a]
41	0	OMe	8 ± 4	0.4 ± 0.1	13 ± 4	1.2 ± 0.3	130 ± 11	14 ± 3	100 ± 5
42	0	NHMe	180[a]	ND[b]	27[a]	ND	ND	ND	ND
43	1	Cyclopropyl	43[a]	4.1[a]	ND	7.1[a]	22[a]	1.3[a]	10[a]
44	1	2-Furyl	110[a]	ND	15[a]	ND	ND	ND	ND
45	1	OMe	2400 ± 137	ND	ND	ND	ND	ND	ND
46	1	NHMe	1.9[a]	ND	ND	2[a]	65[a]	100[a]	5[a]
47	1	NHPr	6 ± 2	4 ± 1	10 ± 3	2.4 ± 0.5	54 ± 3	15 ± 5	24 ± 5
48	1	NHPri	23 ± 5	6 ± 2	11 ± 3	1.9 ± 0.2	64 ± 23	27 ± 12	25 ± 5

[a] $n = 1$.
[b] ND = not determined.

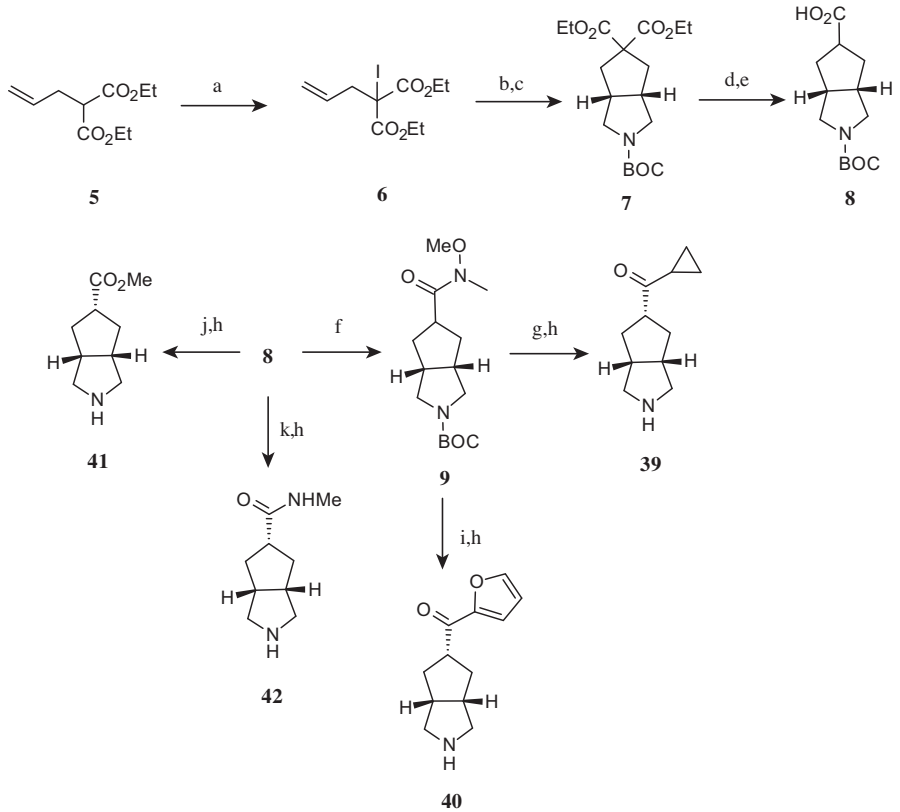

Scheme 1. Reagents and conditions: (a) NaH, NIS; (b) $BocNHCH_2CH{=}CH_2$, $Bu_3SnSnBu_3$, hν; (c) *i*-Pr_2NEt; (d) HCl; (e) $NaHCO_3$, Boc_2O; (f) $MeONHMe{\cdot}HCl$, *i*-Pr_2NEt, HBTU; (g) cyclopropylmagnesium bromide; (h) CF_3CO_2H/CH_2Cl_2; (i) 2-bromofuran, *n*-BuLi; (j) MeOH, DMAP, DCC; (k) *i*-Pr_2NEt, $(COCl)_2$, $MeNH_2$.

methyl ester **41** and methylamide **42**. The *cis*- and *trans*-isomers of the final compounds were separated as N-Boc-derivatives by flash chromatography.

The 7-substituted 3-azabicyclo[3.3.1]nonane (Scheme 2) was obtained by α,α′-annulation of N-protected piperidone **10**.[10] The latter was converted into a pyrrolidine enamine followed by an addition of dibromoisobutyrate. Cyclization occurred via tandem Stork alkylation including subsequent isomerization of the intermediate imminium salt to the enamine. A Wolff–Kishner selective reduction of carbonyl moiety in **11** was accomplished by formation of tosylhydrazone and followed by treatment with sodium cyanoborohydride. Ketones **43**, **44** and amides **46**–**48** were obtained by the same methods as their cyclohomologs, 3-azabicyclo[3.3.0] octane derivatives. 7-Substituted 3-azabicyclo[3.3.1]nonane exists exclusively in *endo*-configuration and preferable boat-chair conformation.

Short chain aliphatic and small alicyclic amides of 3,7-diazabicyclo[3.3.0]octane are generally potent α4β2 nAChR agonists, while their 3,7-diazabicyclo[3.3.1]nonane cyclohomologs only partially activate the receptor (Tables 1 and 2). Incorporation of

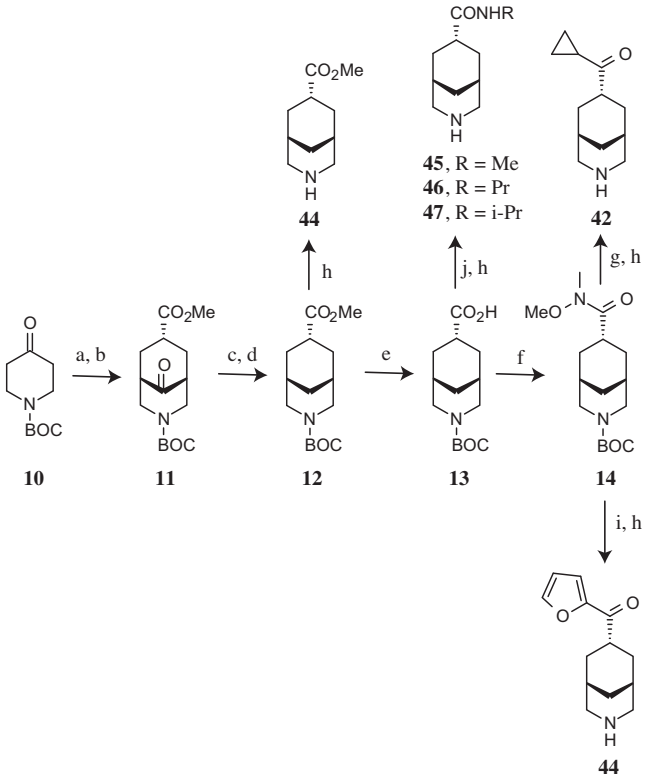

Scheme 2. Reagents and conditions: (a) pyrrolidine; (b) $(BrCH_2)_2CHCO_2Me$, Et_3N; (c) TsN_2H_3; (d) $NaCNBH_3$; (e) LiOH; (f) MeONHMe·HCl, *i*-Pr_2NEt, HBTU; (g) cyclopropylmagnesium bromide; (h) CF_3CO_2H/CH_2Cl_2; (i) 2-bromofuran, *n*-BuLi; (j) *i*-Pr_2NEt, $(COCl)_2$, RNH_2.

electron withdrawing groups in the cyclopropane ring stereospecifically affects α4β2 and α3β4 agonism in opposite directions. Fluorocyclopropyl amide **19** demonstrates elevated α4β2 potency (EC_{50} = 0.19 μM) and diminished α3β4 activation (EC_{50} = 8.4 μM) in comparison with its unsubstituted analog **15**. While all fluoro-substituted amides **16**–**19** show improved α4β2/α3β4 selectivity, compound **19** (α3β4EC_{50}/α4β2EC_{50} = 44) significantly exceeds the selectivity of **15** (α3β4EC_{50}/α4β2EC_{50} = 10). Fluorocyclopropyl amides of 3,7-diazabicyclo[3.3.1]nonane (**25**–**28**) do not gain any selectivity and are equipotent α4β2 partial agonists and α3β4 full agonists. Among methyl-substituted cyclopropyl amides, only compound **22** might be considered as a moderately selective α4β2 agonist. The presence of an annulated diazabicyclo[3.3.0]octane ring, as a cationic pharmacophoric element in the amide series, seems more preferable for activation of the α4β2 nAChR, while the bridged diazabicyclo[3.3.1]nonane ring aincreases α3β4 agonism and interaction with α7 nAChR; especially, for cyclopropane carboxamides. Such tendency culminates in amide **31**, which is the most potent α3β4 nAChR agonist (EC_{50} = 80 nM, E_{max} = 160%) in the series.

Given that enhanced hydrogen bond acceptor strength might improve interaction with α4β2 nAChR, we tested 7-carbonyl derivatives of 3-azabicyclo[3.3.0]octane and 3-azabicyclo[3.3.1]nonane (Table 3). As expected, compound **39** demonstrated increased interaction with the receptor, which is reflected as higher binding affinity (K_i = 0.5 nM) and potency (EC_{50} = 18 nM). However, its cyclohomologous ketone **43** did not follow this trend. The azabicyclo[3.3.1]nonane derivative's slack interaction in comparison with compound **24** might be explained by the drastically altered conformation of the bicyclic scaffold. Unlike 3,7-diazabicyclo[3.3.1]nonane, 3-azabicyclo[3.3.1]nonane exists in a preferable boat-chair conformation with the attached 7-carbonyl moiety exclusively in *endo*-configuration.[10]

Three-dimensional structural evidence of the carbonyl moiety acting as a hydrogen-bond acceptor is illustrated by binding modes predicted via docking the ligands into α4β2 and α3β4 homology models (Figs. 2a and 2b). In both cases, we found that (Figs. 2c and 2d) the hydrogen-bonds contracted by the ligand carbonyl moiety (3.26 and 2.28 Å, respectively) are longer than the ones donated by the cationic center to the backbone carbonyl moiety of the conserved Trp-149 (2.65 and 1.71 Å, respectively). In addition to hydrogen-bonding interactions, docking revealed that cation–π interactions, coulombic interactions, pair-wise lipophilic interactions, and hydrophobic enclosures significantly contribute to the binding free energy for both receptor subtypes.

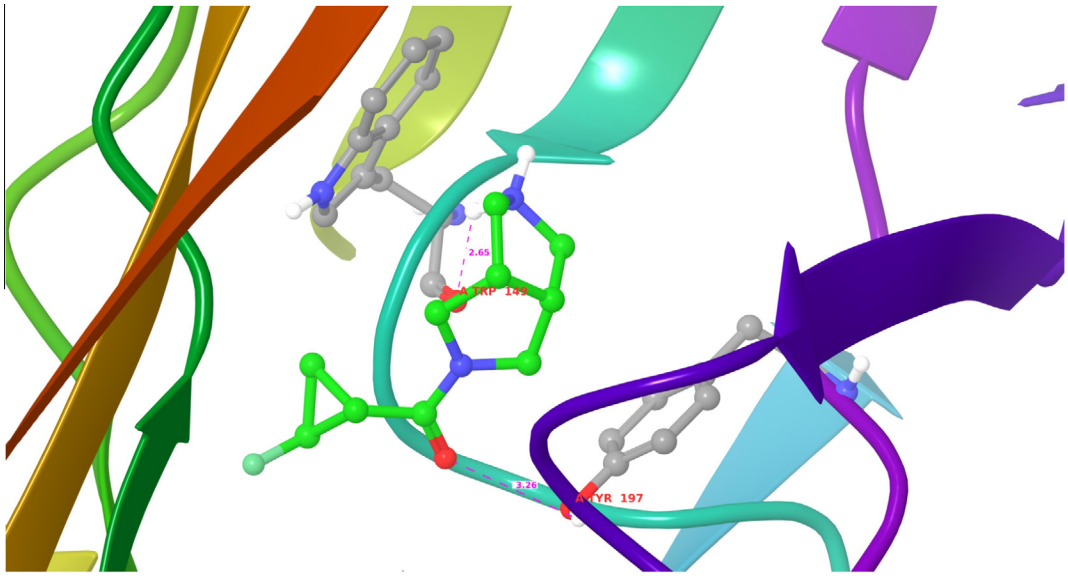

Figure 2a. Calculated best pose of a cyclopropyl carboxamide compound (**16**) docked into a human α4β2 homology model. The ligand is shown by a ball and stick representation and colored green. Trp-149 and Tyr-197 (of the principal face) which are involved in hydrogen-bond interactions with the basic nitrogen and the amide oxygen of the ligand, respectively, are also shown by a ball and stick representations. Hydrogen-bond distances respectively involving the ligand cationic center and the ligand amide group (2.65 and 3.26 Å, respectively) are shown in dotted lines and colored in magenta.

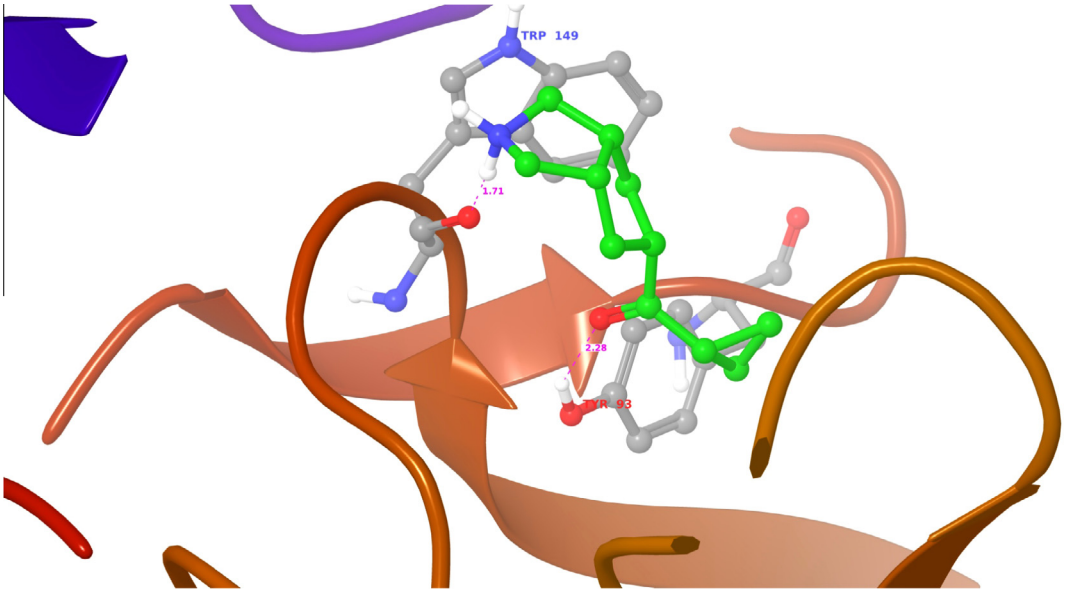

Figure 2b. Calculated best pose an azabicyclic derivative (compound **39**) docked into human α3β4 homology model. The ligand is shown by a ball and stick representation and colored green. Trp-149 and Tyr-93 (of the principal face), which are involved in hydrogen-bond interactions with the basic nitrogen and the carbonyl oxygen of the ligand, respectively, are also shown by a ball and stick representation. Hydrogen-bond distances respectively involving the ligand cationic center and the ligand amide group (1.71 and 2.28 Å, respectively) are shown in dotted lines and colored in magenta.

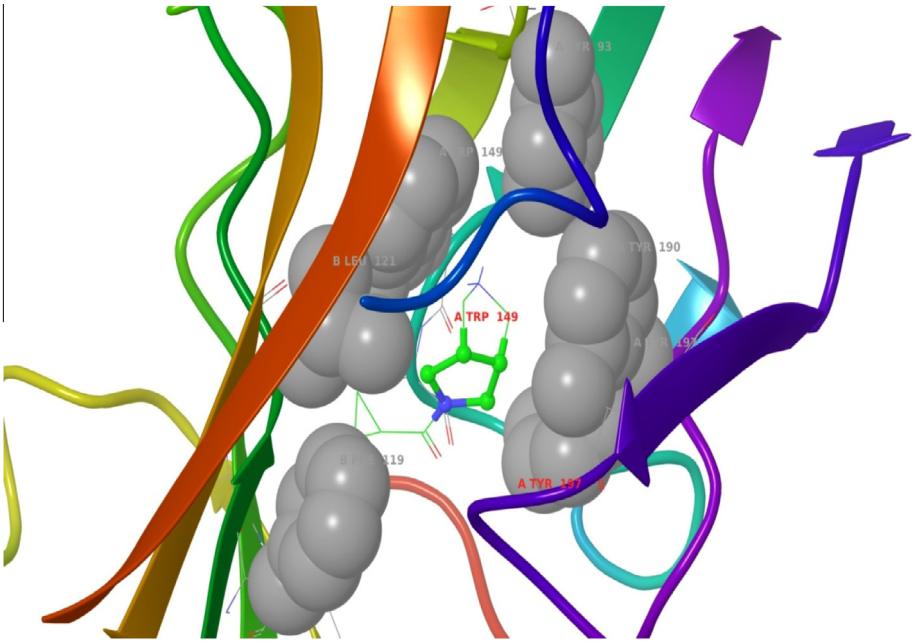

Figure 2c. Best pose of a cyclopropyl carboxamide compound (**16**) docked into human α4β2 nAChR homology model. Compound **16** is colored in green. Part of the molecule, which is involved in hydrophobic enclosure interactions with amino acid residues (shown in space-filling representation), is illustrated in ball and thick stick form, while the remainder of the ligand atoms are shown in thinner stick form.

We have investigated plausible correlations between 140 molecular descriptors for potency and efficacy. Structural, spatial, thermodynamic, topological, and electronic descriptors, as implemented within Pipeline Pilot (Accelrys Inc., San Diego, CA) were used. We have found that compounds with potency $\leqslant$5 μM at the α4β2 receptor subtype can be accurately discriminated from their non-potent counterparts (EC_{50} >5 μM) using the Jurs descriptor J-PPSA_3, with a receiver operating characteristic curve (ROC) score of 0.89 (see Fig. 3). By definition, this descriptor is the atomic charge weighted positive surface area. In other terms, J-PPSA-3 is the sum of the product of solvent-accessible surface area and partial charge for all positively charged atoms. A Roc plot can assist one in understanding the tradeoff between the ability of the descriptor of interest (J-PPSA_3) to identify true positives, that is, potent compounds, and its ability to avoid false positives, that is, non-potent compounds, when J-PPSA-3 is used as a learned model. The closer the Roc score is to 1.0, the better the descriptor is at distinguishing potent from non-potent compounds.

In addition, we found that efficacy at the α4β2 receptor subtype correlates reasonably well with the Jurs descriptor J-FPSA-3

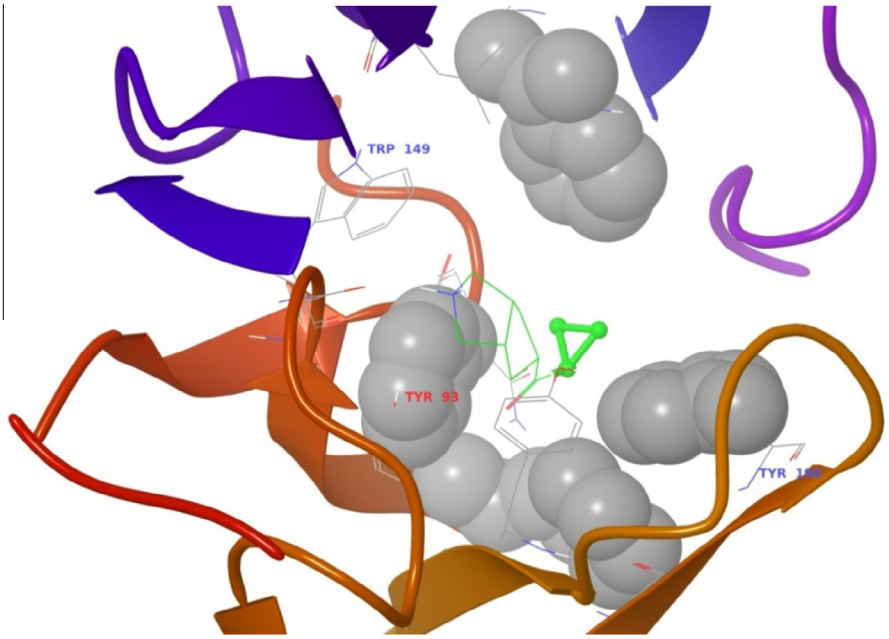

Figure 2d. Best pose of an azabicyclic derivative (**39**) docked into a human α3β4 nAChR homology model. Compound **39** is colored in green. The cyclopropyl moiety, which is involved in hydrophobic enclosures interactions with amino acid residues (shown in space-filling representation), is illustrated in ball and thick stick form, while the remainder of the ligand atoms are shown in thinner stick form.

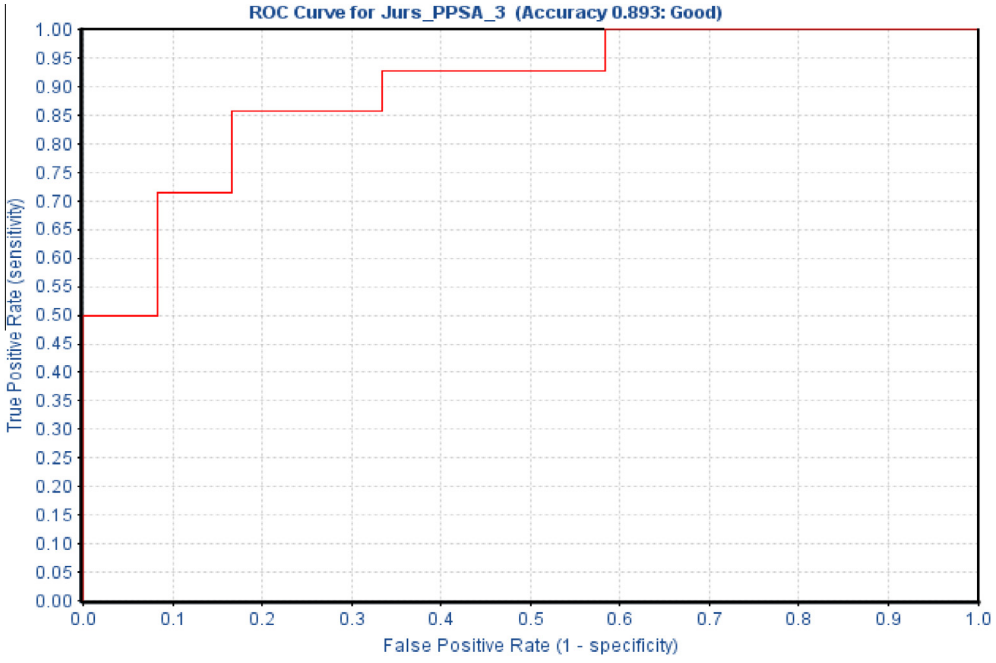

Figure 3. ROC curve for the ability of a model solely based on Jurs-PPSA-3 to discriminate between potent (α4β2 $EC_{50} \leqslant 5$ μM) and non-potent compounds (α4β2 $EC_{50} > 5$ μM).

Table 4
Molecular descriptors of selected nAChR ligands

Compd	EC_{50} (μM)		E_{max} (%)		Radius of gyration	CHI-V3-C	Shadow-XZ	J-FPSA-3 × 10^2
	α4β2	α3β4	α4β2	α3β4				
39	0.018	0.93	120	130	2.96	0.69	48.16	5.73
43	7.1	1.3	22	10	3.17	0.76	51.22	5.27
15	0.47	4.9	110	130	3.08	0.64	47.53	6
24	0.85	1.2	46	160	2.92	0.72	48.12	5.64

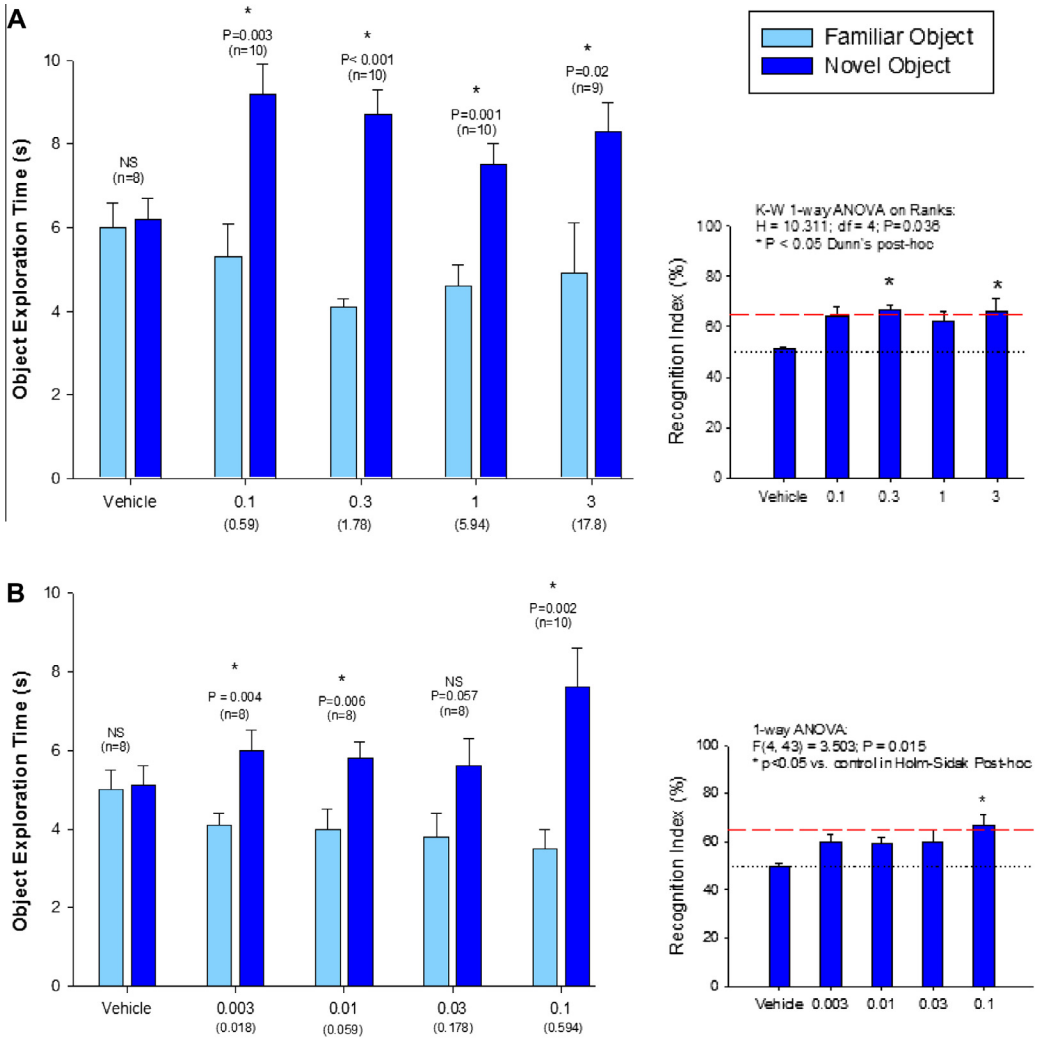

Figure 4. Efficacy of compound **33** in a novel object recognition (NOR) paradigm in rats. Results represent the object recognition time and the recognition index as a function of dose ranges 0.1–3 (A) and 0.003–0.1 (B) following administration of **34** in mg/kg; po (μmol/kg; po).

(r^2 = 0.56), as shown in Figure S1. By definition, J-FPSA-3 is the ratio of the total charge weighted positive surface area to the total molecular solvent-accessible surface area. To further illustrate the influence of physico-chemical properties of compounds on the agonism of this series of compounds, we compared two pairs of compounds (3.3.0 vs 3.3.1) containing a cyclopropyl group. In addition, we compared respective compounds having either an amide group (compounds **15** and **24**) or a ketone group (compounds **39** and **43**) as a hydrogen bond acceptor. Results are shown in Table 4. We found that the increase in potency and efficacy observed at α4β2 in the bicyclo[3.3.0]octane series as compared to the bicyclo[3.3.1]nonane series appears to correlate with a decrease in shadow_XZ and CHI-V-3-C molecular descriptors, which are both related to the shape of the compound. Specifically, Shadow XZ is a shape-based descriptor calculated by projecting the molecular surface onto the XZ plane, whereas CHI-V-3-C is a 3rd order cluster vertex subgraph count index. In addition, the same increase in potency and efficacy seem to correlate directly with an increase in ligand Jurs-FPSA-3. In fact, the pair of bicyclo[3.3.0]octane analogs (**15** and **39**) has the highest values of J-FPSA-3 (0.060 and 0.057, respectively) exhibit the most potent EC_{50} values at α4β2 (0.47 and 0.018 μM). Likewise, the pair of bicyclo[3.3.1]nonane derivatives (**24** and **43**) which exhibit the lowest values of J-FPSA-3 (0.056 and 0.053, respectively) also exhibit the highest values of α4β2 EC_{50} (0.85 and 7.1 μM, respectively). Taken together, these observations suggest that on the whole, the increase in potency and efficacy observed in the bicyclo[3.3.0]octane series results from a molecular shape which promotes more exposure of the positively charged surface areas to the solvent. This is consistent with the docking results which suggested that weaker cations–π interactions and hydrophobic enclosures are observed with the more polar bicyclo[3.3.0]octane derivatives as compared to their diazabicyclo[3.3.1]nonane counterparts. Comparison of molecular descriptors with agonism at the α3β4 subtype suggests that on the whole, the lower the radius of gyration, the more potent and efficacious is the compound, as shown in Table 4. For example, compound **24** has the shortest radius of gyration (2.92) and exhibits the highest value of α3β4 Emax (160%). By contrast, compound **43** has the highest value of radius of gyration (3.17) and exhibits the lowest value of α3β4 Emax (10%). Moreover, the pair of compounds **24** and **39**, which exhibits the shortest pair of values for radius of gyration (2.92 and 2.96, respectively) also exhibit the lowest values of α3β4 EC_{50} (0.93 and 1.2 μM, respectively). Likewise, the pair of compounds **43** and **15**, which exhibit the highest values of radius of gyration (3.17 and 3.08, respectively) also exhibit high values of α3β4 EC_{50} (1.3 and 4.9 μM, respectively). The radius of gyration is defined as the mass-weighted root-mean-square average distance of all atoms in the

molecule from their center of mass. A lower radius of gyration suggests a more spheric-like shape of the compound. By contrast, a higher radius of gyration suggests a more elongated the molecular shape. That the potency and efficacy of compounds at the α4β2 and α3β4 subtypes are dictated by the shape of the compound as suggested by their correlation with shape-based descriptors, Shadow XZ, CHI-V-3_C and radius of gyration, is consistent with ROCS-derived shape analysis. In fact, we have found that Tanimoto shape can discriminate potent compounds (EC_{50} ⩽5 μM) from non-potent compounds (EC_{50} >5 μM) with a Roc (receiver operating characteristic curve) score of 0.82 (see Supplementary data Fig. S2 and S3). The 5 μM cutoff was selected based on compound **4**, also known as AZD1446. This diazabicyclo[3.3.0]octane derivative is a highly selective α4β2 nAChR agonist which is currently being evaluated in clinical trials for the treatment of cognitive disorders associated with psychiatric or neurological disorder. It has an EC_{50} value of 4.9 μM at the human α4β2 nAChR, which led us to choose 5 μM as cuttoff between actives and inactive compounds. Using a cutoff of 5 nM which could discriminate more potent compounds was simply hindered by the fact that none of the compounds reported herein exhibited such highly potent EC_{50} values. Moreover, either using a cutoff of 5 nM (if there were active compounds at such cutoff) or 1.3 μM (which would be based based on compound **34** which has also demonstrated a working memory performance in a novel object recognition test) woulde erronously classify compound **4** has inactive, because its EC_{50} value is greater than 5 nM and 1.3 μM.

To ensure that our shape-based findings were not restricted by the size of the chemical library, we performed a similar study in which we increased the library size by including aromatic bicyclo [3.3.0]octane series and and bicyclo [3.3.1]nonane series contaning furoyl or pyridine moiety, which have been recently reported by Mazurov et al.,[6] Using the same program ROCS, the same EC_{50} cutoff (5 μM) and the same reference (see Fig. S3), we obtained a Tversky shape model with a good roc score of 0.84. This result, shown in Figure S4, was significantly different from a Lingos-derived model (roc score of 0.62) with a *p*-value of 0.001. Besides, due to the fact that functional values could quite vary depending on the source and experimental settings, we increased the EC_{50} cutoff to 10 μM, using this larger and more diverse chemical library. The ROCS software package still produced a reasonable Tversky shape model with a roc score of 0.83, whcih was also significantly superior and different from Lingos-derived model (roc score of 0.63), with a *p*-value of 0.002.

In vitro pharmacological profiling and molecular modeling studies of synthesized compounds indicate that the carbonyl group, as a hydrogen bond acceptor, along with the cationic pharmocophoric element, promote activation of nAChRs, especially, the α4β2 subtype. Moreover, it appears that pyridine, which is a common moiety in nicotinic ligands, or another heterocycle in the molecule can be equivalently replaced by both an exocyclic carbonyl group and a hydrophobic aliphatic group to successfully confer agonism towards the α4β2 nAChR subtype. Since activation of α4β2 nAChR is associated with a cognitive-enhancing effect,[11] we tested aliphatic amide **34** in a novel object recognition (NOR) task (Fig. 4). The object recognition model is based on a rodent's spontaneous tendency to explore novel aspects and ignore familiar aspects of their environment. This pattern of exploratory activity can be used as an index of memory function. Full α4β2 nAChR agonist **34** enhanced working memory in the NOR paradigm in rats at every dose (0.1–3 mg/kg, po) tested in a first experiment. Further exploration of lower doses revealed that compound **34** statistically and significantly increased novel object exploration time at doses as low as 0.003 mg/kg. The maximum percent of recognition index was demonstrated with doses of 0.3 and 3 mg/kg. By comparison, animals treated with vehicle showed no evidence of enhanced memory as subjects spent approximately the same amount of time investigating the novel and familiar objects.

In conclusion, several series of α4β2 nAChR agonists are disclosed, compared, and contrasted. An exocyclic carbonyl moiety, as a hydrogen bond acceptor, is positioned at an optimal distance from a secondary amino group via either a diazabicyclic or an azabicyclic scaffold. Attachments of short chain aliphatic or small alicyclic groups to the carbonyl fragment suffice to promote high binding affinity and activation of nAChRs. Modeling studies suggested that ligand shape plays a key role in contributing to agonism. Tested compound **34** has demonstrated improved working memory performance in a novel object recognition task.

Supplementary data

Supplementary data associated with this article can be found, in the online version, at http://dx.doi.org/10.1016/j.bmcl.2013.04.058.

References and notes

1. Tally, A.; Corringer, P. J.; Guedin, D.; Lestage, P.; Changeux, J. P. *Nat. Rev. Drug Disc.* **2009**, *8*, 733.
2. Sullivan, J. P.; Bannon, A. W. *CNS Drug Rev.* **1996**, *2*, 21.
3. Potter, A.; Corwin, J.; Lang, J.; Piasecki, M.; Lenox, R.; Newhouse, P. A. *Psychopharmacology (Berl., Ger.)* **1999**, *142*, 334.
4. Rowbotham, M. C.; Arslanian, A.; Nothaft, W.; Duan, W. R.; Best, A. E.; Pritchett, Y.; Zhou, Q.; Stacey, B. R. *Pain* **2012**, *153*, 862.
5. Williams, K. E.; Billing, C. B.; Gong, J.; Reeves, K. R. *JAMA* **2006**, *296*, 56.
6. Mazurov, A. A.; Kombo, D.; Miao, L.; Bhatti, B. S.; Strachan, J.-P.; Akireddy, S.; Murthy, S.; Xiao, Y.; Hammond, P.; Zhang, J.; Hauser, T. A.; Jordan, K. G.; Miller, C. H.; Speake, J. D.; Gatto, G. J.; Yohannes, D. *J. Med. Chem.* **2012**, *55*, 9181.
7. Binding to nAChRs was assayed on membranes using standard methods adapted from published literature: (a) Lippiello, P. M.; Fernandes, K. G. *Mol. Pharmacol.* **1986**, *29*, 448; (b) Davies, A. R.; Hardick, D. J.; Blagbrough, I. S.; Potter, B. V.; Wolstenholme, A. J.; Wonnacott, S. *Neuropharmacology* **1999**, *38*, 679. Functional data were obtained according to methods described in Ref. 6.
8. Flynn, D. L.; Zabrowski, D. L. *J. Org. Chem.* **1990**, *55*, 3673.
9. ^{1}H NMR ($CDCl_3$, 300 MHz): δ 3.69 (s, 3H), 3.60–3.42 (m, 2H), 3.36–3.05 (m, 3H), 3.18 (s, 3H), 2.82–2.57 (m, 2H), 2.08–2.02 (m, 2H), 1.82–1.65 (m, 2H), 1.46 (d, 9H); MS (*m*/*z*: 299 (M+1), 243 (M+1-56). **39**, ^{1}H NMR (CD_3OD, 300 MHz): δ 3.59–3.40 (m, 2H), 3.37–3.29 (m, 1H), 3.02–2.90 (m, 4H), 2.16–2.03 (m, 3H), 1.87–1.80 (m, 2H), 0.96–0.91 (m, 4H); MS (*m*/*z*): 180 (M+1). **41**, ^{1}H NMR (CD_3OD, 300 MHz): δ 3.74 (s, 3H), 3.57–3.32 (m, 2H), 3.22–3.16 (m, 2H), 3.05–2.88 (m, 3H), 2.38–2.03 (m, 2H), 1.83–1.61 (m, 2H); MS (*m*/*z*): 170 (M+1). **47**, ^{1}H NMR (CD_3OD, 300 MHz): δ 3.25–3.10 (m, 4H), 2.85–2.75 (m, 1H), 2.40–2.18 (m, 4H), 1.85–1.42 (m, 8H), 0.95 (t, 3H); MS (*m*/*z*): 211 (M+1).
10. Speckamp, W. N.; Dijkink, J.; Dekkers, A. W. J. D.; Huisman, H. O. *Tetrahedron* **1971**, *27*, 3143.
11. Levin, E. D.; McClernon, F. J.; Rezvani, A. H. *Psychopharmacology* **2006**, *184*, 523.